



ORIGINAL ARTICLE

Extracellular ATP and cAMP signaling promote Piezo2-dependent mechanical allodynia after trigeminal nerve compression injury

Zhaoke Luo^{1,2} | Xinyue Liao^{1,2} | Lili Luo^{1,2} | Qitong Fan^{1,2} | Xiaofen Zhang^{1,2} | Yuefeng Guo^{1,2}  | Feng Wang^{1,2} | Zucheng Ye^{1,2} | Daoshu Luo^{1,2} 

¹Key Laboratory of Brain Aging and Neurodegenerative Diseases of Fujian Province, Laboratory of Clinical Applied Anatomy, the School of Basic Medical Sciences, Fujian Medical University, Fuzhou, China

²Department of Human Anatomy, the School of Basic Medical Sciences, Fujian Medical University, Fuzhou, China

Correspondence

Daoshu Luo and Zucheng Ye, Department of Human Anatomy, The School of Basic Medical Sciences, Fujian Medical University, No. 1 Xuefu North Road, University Town, Fuzhou, China.
Email: luods2004@fjmu.edu.cn; zcye@u.washington.edu

Funding information

This work was funded by the National Natural Science Foundation of China (Grant number: 82171213), United Fujian Provincial Health and Education Project for Tackling the Key Research P.R. China (Grant number: 2019WJ26), and Startup Fund for scientific research, Fujian Medical University (Grant number: 2020QH1001)

Abstract

Trigeminal neuralgia (TN) is a type of severe paroxysmal neuropathic pain commonly triggered by mild mechanical stimulation in the orofacial area. Piezo2, a mechanically gated ion channel that mediates tactile allodynia in neuropathic pain, can be potentiated by a cyclic adenosine monophosphate (cAMP)-dependent signaling pathway that involves the exchange protein directly activated by cAMP 1 (Epac1). To study whether Piezo2-mediated mechanotransduction contributes to peripheral sensitization in a rat model of TN after trigeminal nerve compression injury, the expression of Piezo2 and activation of cAMP signal-related molecules in the trigeminal ganglion (TG) were detected. Changes in purinergic P2 receptors in the TG were also studied by RNA-seq. The expression of Piezo2, cAMP, and Epac1 in the TG of the TN animals increased after chronic compression of the trigeminal nerve root (CCT) for 21 days, but Piezo2 knockdown by shRNA in the TG attenuated orofacial mechanical allodynia. Purinergic P2 receptors P2X4, P2X7, P2Y1, and P2Y2 were significantly up-regulated after CCT injury. In vitro, Piezo2 expression in TG neurons was significantly increased by exogenous adenosine 5'-triphosphate (ATP) and Ca^{2+} ionophore ionomycin. ATP pre-treated TG neurons displayed elevated $[\text{Ca}^{2+}]_i$ and faster increase in responding to blockage of $\text{Na}^+/\text{Ca}^{2+}$ exchanger by KB-R7943. Furthermore, mechanical stimulation of cultured TG neurons led to sustained elevation in $[\text{Ca}^{2+}]_i$ in ATP pre-treated TG neurons, which is much less in naïve TG neurons, or is significantly reduced by Piezo2 inhibitor GsMTx4. These results indicated a pivotal role of Piezo2 in peripheral mechanical allodynia in the rat CCT model. Extracellular ATP, Ca^{2+} influx, and the cAMP-to-Epac1 signaling pathway synergistically contribute to the pathogenesis and the persistence of mechanical allodynia.

Abbreviations: ATF3, activating transcription factor 3; ATP, adenosine 5'-triphosphate; BSA, bovine serum albumin; cAMP, cyclic adenosine monophosphate; CCT, chronic compression of the trigeminal nerve root; cDNA, complementary DNA; CGRP, calcitonin gene-related peptide; CREB, cAMP-responsive element-binding; Ct, cycle threshold; DEGs, differentially expressed genes; DMEM, Dulbecco's modified eagle medium; DRG, dorsal root ganglion; EDTA, Ethylene Diamine Tetraacetic Acid; ELISA, enzyme-linked immunosorbent assay; Epac1, exchange protein directly activated by cAMP 1; FBS, fetal bovine serum; FDR, false discovery rate; FPKM, fragments per kilobase of exon model per million mapped reads; GAPDH, glyceraldehyde-3-phosphate dehydrogenase; GPCRs, G-protein-coupled receptors; GTP, guanosine triphosphate; HBSS, HEPES-buffered saline solution; HEPES, N-(2-Hydroxyethyl) piperazine-N'-(2-ethanesulfonic acid); IASP, International Association for the Study of Pain; NCX, $\text{Na}^+/\text{Ca}^{2+}$ exchanger; NEFH, neurofilament, heavy polypeptide; NSE, neuron-specific enolase; P2Rs, purinergic 2 receptors; PBS, phosphate-buffered saline; PCR, polymerase chain reaction; Rap1, rhoGTPase-1; RIPA, radioimmunoprecipitation assay; RNA-seq, ribonucleic acid sequencing; RSEM, RNA-seq by expectation maximization; SD, standard deviation; SDS-PAGE, sodium dodecyl sulfate polyacrylamide gel electrophoresis; SEM, standard error of mean; shRNA, short hairpin ribonucleic acid; TG, trigeminal ganglion; TN, trigeminal neuralgia; TREZ, trigeminal root entry zone.

Zhaoke Luo and Xinyue Liao contributed equally to this work.

KEYWORDS

ATP, Ca^{2+} homeostasis, cAMP signaling pathway, mechanical allodynia, Piezo2, trigeminal neuralgia

1 | INTRODUCTION

Trigeminal neuralgia (TN), severe neuropathic pain characterized by paroxysmal pain in the orofacial area, can be triggered by slight touch or other mild mechanical stimuli at a specific trigger zone on the face (Cruccu et al., 2016; Jones et al., 2019). Although microvascular compression on the trigeminal root entry zone (TREZ) is a common etiology in most primary TN cases, the pathogenesis of TN remains unknown. Mechanical hypersensitivity in the trigeminal nerve is thought to play a crucial role in the pathophysiology of TN, but no systematic research is available evidence to elucidate the mechanisms.

Piezo2 was recently identified as an ion channel that mediates mechanosensory transduction and implicated in mechanical hyperalgesia and allodynia (Murthy et al., 2018a). Piezo2 was shown to be extensively expressed in Merkel cells, dorsal root ganglion (DRG), and trigeminal ganglion (TG) neurons in rodents, in addition to its involvement in human mechanosensation (Chesler et al., 2016; Szczot et al., 2018). Piezo2 was reported to mediate injury-induced tactile pain in mice and humans, and Piezo2 is an essential transduction ion channel for gentle touch and tactile allodynia (Eijkelkamp et al., 2013). However, the exact molecular mechanisms of mechanical hypersensitivity and allodynia remain poorly understood. A previous study reported that a cyclic adenosine monophosphate (cAMP) sensor, exchange protein directly activated by cAMP 1 (Epac1), contributed to the development of allodynia in a chronic constriction injury animal model, and Epac1 signaling could evoke mechanical allodynia in a manner involving Piezo2-mediated mechanotransduction (Eijkelkamp et al., 2013). Epac1 is a guanine nucleotide exchange factor that activates Rap1, a small GTP-binding protein of the Ras family of GTPases. Rap1 modulates Piezo2 mediated currents to participate in mechanical allodynia (Jia et al., 2013a).

It is well known that adenosine 5'-triphosphate (ATP) is released after nerve injury in several neuropathic pain animal models (Liang et al., 2019; Masuda et al., 2016). ATP acts as an extracellular ligand that activates purinergic 2 receptors (P2Rs) on the cell membrane (Bernier et al., 2018; Burnstock, 1972). P2X receptors are permeable to Na^+ , K^+ , and Ca^{2+} ions (Burnstock, 2012; Schmid & Evans, 2019), and P2Y receptors are G-protein-coupled receptors (GPCRs). The Ca^{2+} -dependent signaling cascade has been implicated in the regulation of Piezo2 activation (Borbiro et al., 2015). Moreover, extracellular ATP induces the activation of several intracellular signaling pathways, including the cAMP pathway (Petit et al., 2009; Zimmermann, 2016). However, the involvement and relationships between extracellular ATP, intracellular Ca^{2+} , cAMP, and the expression and function of Piezo2 have not been systemically investigated.

Although the role of Piezo2 in animal models of neuropathic pain and the interaction of Piezo2 and cAMP signaling have been

mentioned in some studies, the molecular mechanism by which TN is induced by chronic compression of the trigeminal nerve root (CCT) injury in animal models remains largely unknown. Combining a well-established in vivo model and an in vitro model of mechanical stimulation, we investigated the role of Piezo2 in the regulation of peripheral sensitization in a TN rat model.

2 | MATERIALS AND METHODS

2.1 | Animals

Adult male Sprague-Dawley rats (160 ± 20 g; RGD Cat# 13525002, RRID:RGD_13525002) were obtained from the Experimental Animal Center of Fujian Medical University. The animals were housed on a 12:12-h light-dark cycle at constant room temperature ($22 \pm 2^\circ\text{C}$) with food and water provided ad libitum. All experimental procedures were approved by the Animal Care and Use Committee of Fujian Medical University (ethical approval reference number: LLSLBH-20210601-003) and followed the guidelines of the International Association for the Study of Pain (IASP). The study was not pre-registered. G*Power software (G*Power 3.1.9.7, means: difference between two independent means, two tails) was used to verify the Power of the behavior test. The α err prob was set at 0.05, and the sample size of each group was 4. The effect size d was 3.444 which was determined by mean and SD of the two groups (group 1: mean 3.454, SD 0.305; group 2: mean 2.344, SD 0.429). As the Power was 0.980 after calculation, six rats in each group were used for the behavior test in this study.

Our previous studies indicate that at 21 days after the operation, rats underwent CCT displayed stable and prominent allodynia (Luo et al., 2012, 2019), we chose 21 days as time for tissue harvesting. Rats were anesthetized with sodium pentobarbital (200 mg/kg, i.p.) and sacrificed, followed by appropriated tissue preparation procedures for immunohistochemistry, western blot, Elisa, qPCR, and RNA-seq, respectively. The graphical time-line for animal experiments are described in Figure 1.

2.2 | TN animal model and TG shRNA injection

A total number of 64 male rats were used in this study. Rats were marked in the tails with permanent marker and randomly divided into five groups by simple randomization (table of random digit), with a final number of 48 rats included in the results: the naïve group ($n = 6$), TN group ($n = 15$), sham group ($n = 15$), TN + Piezo2 shRNA group ($n = 6$), and TN + scramble shRNA group ($n = 6$). The experimenters were blinded to the treatment during behavioral and biochemical assessments.

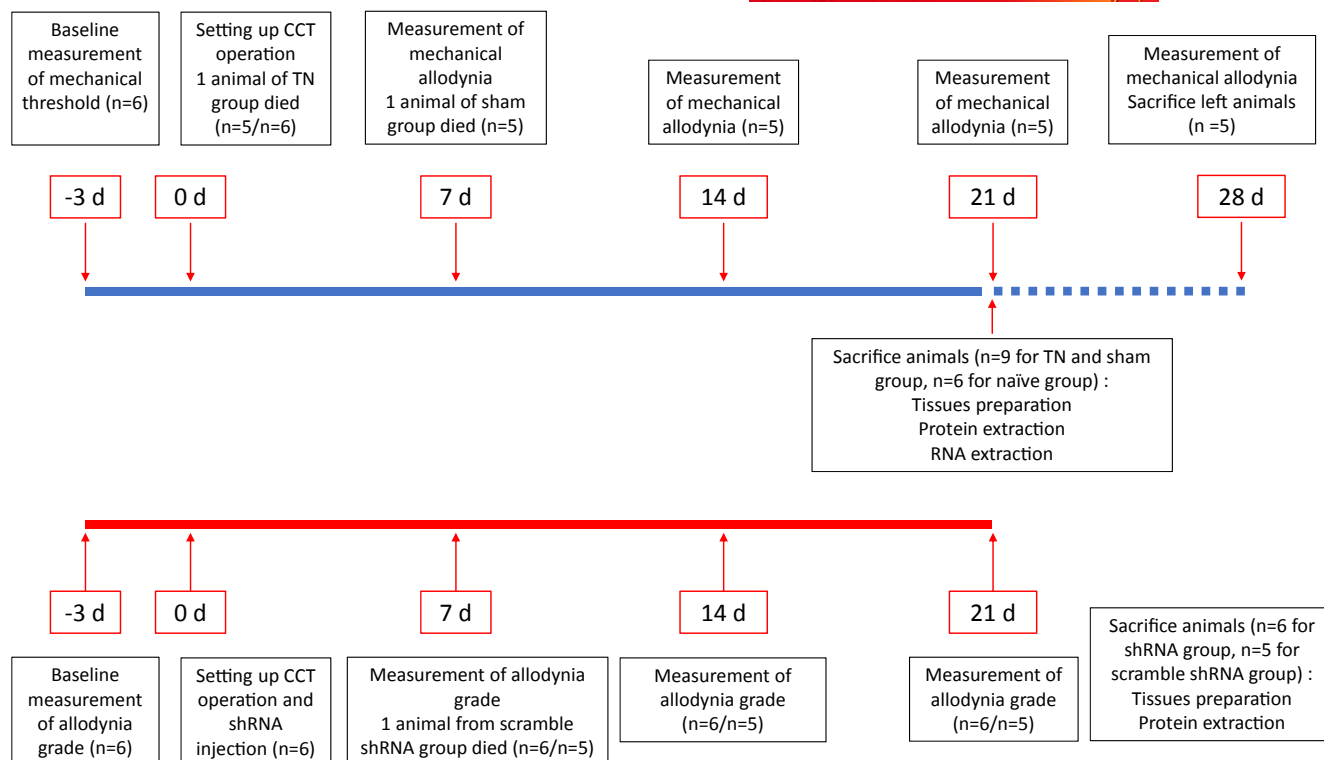


FIGURE 1 The graphical timeline for animal experiments. The blue line corresponds to the timeline of the experiments, including the naïve group, the sham group, and the trigeminal neuralgia (TN) group. The red line corresponds the timeline of experiments on the *Piezo2* shRNA group and the scramble shRNA group

An animal model of TN induced by CCT was established with a modified method based on the previously described protocol (Lin et al., 2018). For the TN group, rats were anesthetized with sodium pentobarbital (40 mg/kg, *i.p.*), and an anterior-posterior curve skin incision was made above the right eye to expose the right infraorbital nerve traveling through the infraorbital groove. A homemade metal conduit with the outside diameter of 0.6 mm and inside diameter of 0.5 mm, slightly curved at the end, was slowly pushed into the intra-calvarium from the inferior orbital fissure to reach the TREZ, then a 0.4-mm nylon wire was pushed along the metal conduit to compress the TREZ. For the sham group, the right infraorbital nerve was exposed without nylon wire compression of the trigeminal nerve. The incision was closed using silk sutures and treated with erythromycin ointment after operation. Rats that did not undergo operation were set as the naïve group. When sacrificed for tissue harvesting, all CCT rats were carefully checked for the location of the nylon wire, those with the nylon wire misplaced from the TREZ were considered as CCT failure. A total number of four rats were categorized as CCT failure and excluded from the results.

shRNA targeting murine *Piezo2* (GenBank accession: XM_225880.10; 5'-CAA TCT TCA CTG CTG GGC ACC TGA T-3'; HANBIO Cat# HBLV-r-PIEZO2 shRNA2-ZsGreen-PURO, Shanghai, China) and a scrambled shRNA (5'-TTC TCC GAA CGT GTC ACG T-3'; HANBIO Cat# HBLV-ZsGreen-PURO) were designed and inserted into the lentiviral vector pHBLV by the U6 promoter (HANBIO Cat# hU6-MCS-EF1-ZsGreen-T2A-puromycin). The lentiviruses

(2×10^5 TU, 2 μ l) were injected into the TG using a 24-G needle (BD) from the infraorbital foramen during CCT. Six rats were excluded from the results due to postmortem revealing of incorrect injection site and/or failure in reducing *Piezo2* expression.

Three rats died during the operation, another three died at 1–20 days after operation. To minimize animal pain in procedures, all the rats were handled gently and returned to their familiar environment as soon as possible after operation or behavior test. No pain medication was given after the surgical operation to avoid interfering with behavior tests.

2.3 | TG neuron primary culture and drug administration

Neonatal Sprague-Dawley rats (1–3 days) were exposed to 3% isoflurane, sterilized with 75% alcohol, and sacrificed. TG tissues were carefully harvested and collected in ice-cold high-glucose DMEM (Invitrogen Cat# C11995500BT). Isolated TG tissues were digested with 1 ml of trypsin-EDTA (0.25%; Invitrogen Cat# 25200-056) mixed with 1 ml of type 1 collagenase (2 mg/ml; Worthington Cat# LS004194) in DMEM at 37°C for 20 min, followed by mechanical trituration. Digestion was terminated with DMEM/F12 medium (1:1; Invitrogen Cat# 11330032) containing 10% (v/v) fetal bovine serum (Invitrogen Cat# 10099141), and centrifuged at 174.4 g for 10 min. After the supernatant was removed, TG neurons were suspended and

seeded onto cell culture dishes pre-coated with poly-D-lysine (Solarbio Cat# P2100) in DMEM/F12 (1:1) culture medium supplemented with 10% (v/v) fetal bovine serum (FBS) and penicillin (100 U/ml) and streptomycin (100 µg/ml; HyClone Cat# SV30010) for 4 h. Then, the medium was replaced with neurobasal (Invitrogen Cat# 21103-049) +2% (v/v) B27 (Invitrogen Cat# 17504-044) neuronal medium for 72 h. TG neuronal cultures from the same preparation were divided into three groups by simple randomization (draw lots) and followed with different drugs were then administered to the primary cultured TG neurons based on their grouping: ATP (1–3 mM; Sigma Cat# ATPD-RO), calcium ionophore ionomycin (500 nM; Tocris, Cat#1704) was then administered to the primary cultured TG neurons and incubated for 1 h, and the medium was exchanged for fresh culture medium. The TG neurons in all the groups were cultured for an additional 72 h before immunocytochemical assays or Ca^{2+} imaging experiments. A total number of 40 neonatal rats were used in TG neuron culturing and subsequent immunohistochemistry and imaging experiments.

2.4 | Tissue preparation and immunohistochemistry

The tissues of the trigeminal nerve root and TG on the right side were harvested after transcardial perfusion through the left ventricle with buffered 4% (w/v) paraformaldehyde and then cryoprotected with a 30% (w/v) sucrose solution in 0.1 M phosphate buffer for 24 h at 4°C. Serial longitudinal sections were cut at a thickness of 10 µm using a cryostat microtome (Leica CM1950).

For immunofluorescence staining, the slices were blocked with QuickBlock™ Blocking Buffer (Beyotime Cat# P0260) for 1 h and then incubated overnight at 4°C with the following primary antibodies: mouse anti-ATF3 (1:100; Santa Cruz Cat# sc-81189, RRID:AB_2058591), rabbit anti-Piezo2 (1:400; Novus Cat# NBP1-78538, RRID:AB_11029076), mouse anti-NSE (1:200; Proteintech Cat# 66150-1-Ig, RRID:AB_2883272), goat anti-CGRP (1:200; Abcam Cat# ab36001, RRID:AB_725807), and chicken anti-NEFH (1:10000; Abcam Cat# ab4680, RRID:AB_30456). After rinsing with 0.01 M phosphate-buffered saline (PBS), the slices were further incubated with donkey anti-goat Alexa Fluor 488 (1:1000; Invitrogen, Cat# A-11055, RRID:AB_2534102), donkey anti-rabbit Alexa Fluor Plus 594 (1:1000; Invitrogen, Cat# A32754, RRID:AB_2762827), goat anti-rabbit Alexa Fluor Plus 555 (1:1000; Invitrogen, Cat# A32732, RRID:AB_2633281), goat anti-mouse Alexa Fluor Plus 647 (1:1000; Invitrogen, Cat# A32728, RRID:AB_2633277), or goat anti-chicken Alexa Fluor 647 (1:1000; Invitrogen, Cat# A-21449, RRID:AB_2535866) at room temperature ($24 \pm 2^\circ\text{C}$) for 1 h. Fluorescence images were captured with a confocal microscope (Leica TCS SP8).

2.5 | Immunocytochemistry

TG neurons were cultured on glass-bottom cell culture dishes, fixed with 4% paraformaldehyde at 4°C for 15 min. Citrate antigen

retrieval was performed, then the fixed cells were blocked with 5% (w/v) bovine serum albumin (BSA) (Phygene Cat# PH0420) for 60 min. Then, the cells were incubated overnight at 4°C with the following primary antibody: rabbit anti-Piezo2 (1:200; Novus Cat# NBP1-78538, RRID:AB_11029076). After rinsing with 0.01 M PBS, the cells were further incubated with goat anti-rabbit Alexa Fluor Plus 555 (1:1000; Invitrogen, Cat# A32732, RRID:AB_2633281) or goat anti-chicken Alexa Fluor 647 (1:1000; Invitrogen, Cat# A-21449, RRID:AB_2535866) at room temperature ($24 \pm 2^\circ\text{C}$) for 1 h. Images were collected using a Leica TCS SP8 confocal microscope.

Fluorescence intensity was determined using Image J software with background subtracted in immunohistochemistry or immunocytochemistry experiments, yielding the average intensity of the region of interest (ROI) matching individual TG neurons. When determining the immunofluorescent intensity of the cell membrane and cytoplasm, each cell had three linear segments of the cell membrane in the length of 2–3 µm quantified and averaged for cell membrane, or three circles with the diameter of 2–3 µm quantified and averaged for the cytoplasm.

2.6 | Measurement of mechanical allodynia

Behavior tests were performed from 2 to 4 pm at 3 days before CCT operation, 7 days post-operation, 14 days post-operation, and 21 days post-operation (28 days post-operation for testing mechanical threshold of TN and sham group). Animals were habituated to the testing environment daily for 3 days before baseline testing, then were placed in mesh metal boxes and adapted for 30 min before the examination. To assess the mechanical threshold, von Frey filaments (Aesthesio) were used to evaluate the orofacial mechanical threshold. The testing procedure was modified from a previously described protocol (Luo et al., 2012). Briefly, each von Frey filament was applied five times, and another new stimulus was applied only when the rat resumed relaxation at least 30 s after the preceding stimulus. Stimulation always began with the filament that produced the lowest force and stopped when the mechanical threshold was found around the vibrissa pad area of the rats.

To measure mechanical allodynia, a 0.07 g von Frey filament was used to evaluate orofacial mechanical allodynia of the trigeminal nerve territory. Noxious behaviors were scored as follow: the rat did not stir or only looked around, score of 0; the rat responded gently or shrunk its face, score of 1; the rat quickly shielded its face or lifted its paw slightly, score 2; the rat showed swift, evasive behavior or lifted its paw and wiped its face, a score of 3; or the rat wiped its face and lifted its paw, a score of 4 (Jiang et al., 2021).

2.7 | Western blot analysis

The ipsilateral TG tissues from each animal were homogenized in ice-cold radioimmunoprecipitation assay (RIPA) lysis buffer (Solarbio Cat# MA0151) and then centrifuged at 12 000 g for 10 min at 4°C.



For TG tissue culture, proteins were extracted by the addition of RIPA lysis buffer to each well, and the samples were then centrifuged at 12 000 g. The protein concentration was measured with a BCA kit (Beyotime Cat# P0010). Equal amounts of protein were separated by electrophoresis on 6% polyacrylamide SDS-PAGE gels and transferred onto polyvinylidene difluoride membranes (Merek Cat# 03010040001). The membranes were blocked with 5% (weight/vol) non-fat milk for 1 h at room temperature ($24 \pm 2^\circ\text{C}$) and then incubated overnight at 4°C with the following primary antibodies: rabbit anti-Piezo2 (1:500; Novus Cat# NBP1-78538, RRID:AB_11029076) and rabbit anti-GAPDH (1:10000; Bioworld Cat# AP0066, RRID:AB_2797448) or mouse anti- β tubulin (1:10000; Bioworld Cat# BS1482 M). The membranes were incubated with horseradish peroxidase-conjugated goat anti-rabbit IgG (H+L) (1:10000; Bioworld BS13278, RRID:AB_2773728) or goat anti-mouse IgG (H+L) (1:10000; Bioworld Cat# BS12478, RRID:AB_2773727) secondary antibody at room temperature ($24 \pm 2^\circ\text{C}$) for 2 h. Protein bands were visualized with Immobilon Western Chemiluminescent Reagent (Millipore Cat# 1925902) and a ChemiDoc™ Imaging System (Bio-Rad). Images were analyzed by Image Lab 6.0 (Bio-Rad).

2.8 | RNA sequencing

The ipsilateral TG and part of its projection to TREZ were harvested and immediately frozen in liquid nitrogen. Tissues were subsequently used for RNA sequencing (RNA-seq) analysis (Beijing Genomics Institute, BGI). cDNA library construction and sequencing were performed with the BGISEQ-500 platform (MGI, Shenzhen, China). High-quality reads were aligned to the rat reference genome using Bowtie2. The differential expression genes were recognized with the DESeq package with discriminant to eliminate the irrelevant genes. Expression levels for each of the genes were normalized to fragments per kilobase of exon model per million mapped reads (FPKM) using RNA-seq by expectation maximization (RSEM). Differentially expressed genes (DEGs) were identified between samples, and clustering analysis and functional annotation were performed. Genes with a ≥ 1.0 -fold change in expression and a false discovery rate (FDR) of ≤ 0.05 were considered as a statistically significant difference in expression. Bioinformatic analysis was performed using the OmicStudio tools at <https://www.omicstudio.cn/tool>.

2.9 | mRNA isolation and real-time qPCR

The ipsilateral TG tissues were isolated, and total RNA was isolated with TRIzol reagent (Invitrogen Cat# 155596026). Reverse transcription was performed with 1 mg of RNA by using the Prime Script™ RT Reagent Kit (Vazyme Biotech Cat# R222-01). Real-time qPCR was performed with SYBR Green PCR Master Mix (Vazyme Biotech Cat# Q311-02) in a CFX96™ Real-Time PCR Detection System (Bio-Rad). The primer pairs are listed in Table 1. PCR amplification was performed at 95°C for 30 s, followed by 40 cycles of thermal cycling

TABLE 1 Primer sets used for qPCR

Gene	Primer sequence	Amplicon size (bp)
<i>Piezo2</i>	5'-ACACCATGCTGGTGCTCATC-3' 3'-AGGGTGGGCTAACCTGTAGA-5'	278
<i>Epac1</i>	5'-GTGTTGGTGAAGGTCAATTCTG-3' 3'-CCACACCACGGGCATC-5'	64
<i>P2rx2</i>	5'-ACTGCTCTGACCTCCATC-3' 3'-TCTCTAGGACTGCCTTAGC-5'	489
<i>P2rx4</i>	5'-GATGGCTACTGCGTCTGTCA-3' 3'-GCAGAAGCAGGAGGATCTTG-5'	157
<i>P2rx7</i>	5'-GACAAACAAAGTCACCCGGAT-3' 3'-CGCTCACCAAAGCAAAGCTAAT-5'	101
<i>P2ry1</i>	5'-AGGTCAAGAAGAAGCAACAT-3' 3'-CAGCAGATAGCAACAAGGA-5'	198
<i>P2y2</i>	5'-GTAGAATCGCAAGGTGACT-3' 3'-GCAGATGGCAGAGATAACA-5'	269
<i>P2y6</i>	5'-CGGTCATCGGCTTCTTGCTTCC-3' 3'-CCTTGCTGCGACGCTCTTGG-5'	120
<i>P2ry12</i>	5'-CTTCGTTCCCTTCCACTTTG-3' 3'-AGGGTGCTCTCCTTACGTA-5'	108
<i>P2ry14</i>	5'-TTCAAGTCTCACCTCAAGTC-3' 3'-AACGGCTGGCATAAGAAG-5'	266
<i>Gapdh</i>	5'-ACGGCAAGTTCAACGGCACAG-3' 3'-GAAGACGCCAGTAGACTCCACGAC-5'	247

at 95°C for 10 s, 50°C for 30 s, and 95°C for 15 s. *Gapdh* was used as an endogenous control to normalize differences in total mRNA levels. Melt curves were prepared upon completion of the cycles to ensure that non-specific products were absent. Quantification was performed by subtracting target gene cycle threshold (Ct) values with the *Gapdh* Ct value and then analyzed with the $2^{-\Delta\Delta\text{Ct}}$ method for a normalized value of gene expression against the sham group.

2.10 | ELISA for cAMP

cAMP activation assay was measured using a cAMP assay kit (Abcam Cat# ab138880) according to the manufacturer's instructions. Ipsilateral TG tissue samples were harvested from the TN group and sham group 21 days after operation for these experiments. The fluorescence of the end product was measured at $\text{Ex/Em} = 540/590 \text{ nm}$ using a Tecan Spark 20 M microplate reader (Tecan Trading AG, Switzerland).

2.11 | Ca^{2+} imaging and mechanical stimulation

Ca^{2+} imaging was performed on a Leica DMI 6000B fluorescent microscope as has been previously reported (Yao et al., 2014) with some modification. Briefly, TG neurons cultured in glass-bottomed

confocal dish (7–12 DIV) were loaded with Fura-2-am (10 μ M; Invitrogen Cat# F1201) in cultured medium (Neurobasal +2% (v/v) B27) for 45 min, then gently replaced with 1.5 ml of a mixture (v/v 1:2, pre-warmed to 37°C) of culture medium and Hepes-buffered saline solution (HBSS), consisted of 126.25 mM NaCl, 2.0 mM CaCl_2 , 3.0 mM KCl, 1.25 mM NaH_2PO_4 , 2.0 mM MgSO_4 , 10 mM glucose, and 25 mM HEPES. HBSS was adjusted to pH 7.40 by NaOH and 0.22 μ m filtered. To reduce heat loss, 40 \times oil objective was kept at 37°C using a TPIE-LH lens heater (Tokai Hit, Japan). Cells were excited at 340 and 380 nm using an ultraviolet light source (Lambda XL lamp, Sutter Instrument), digitized images were collected at 0.1 Hz using an ORCA-Flash 4.0 V3 sCMOS camera (Hamamatsu). Metafluor program (Molecular Devices) was used to coordinate the light source, microscope, and camera for data acquisition and for imaging analysis. KB-R7943 (20 μ M; MCE Cat# HY-15415) were applied to block $\text{Na}^+/\text{Ca}^{2+}$ exchanger (NCX) in some of experiments.

Glass beads at diameters of 50–100 μ m (Polysciences Cat# 15926) were used as mechanical stimulation. Fifteen milligram of glass beads in a volume of 30 μ l of HBSS was gently released from a pipet-tip (0–200 μ l) at 1.0 cm above the cells. Released glass beads traveled through the layer of medium, delivered an initial mechanical shock then sit still above the TG neurons, yielding a continuous mechanical stimulation.

2.12 | Statistical analyses

In the histogram, data are expressed as the mean \pm SEM. Box-whisker plots show 25th-to-75th percentiles around the median, with whiskers showing the maximum and minimum of these data. All data presented represent the mean of at least three replicates of independent samples. All statistical analyses were performed using GraphPad Prism 9 (GraphPad Software, Inc.). The Student's two-tailed *t*-test was used for two-group comparisons, and one-way ANOVA or two-way repeated-measures ANOVA was used for multiple comparisons, followed by Bonferroni's test. $p < 0.05$ was used to indicate statistical significance.

The study was exploratory. All experiments were performed and repeated according to the same time schedule. Normality was determined using the Shapiro–Wilk normality test. No test for outlier identification was conducted on the data and no data point was excluded from the statistical analysis.

3 | RESULTS

3.1 | Piezo2 was up-regulated in the TG neurons after CCT

CCT induced orofacial mechanical allodynia from 7 to 28 days after operation, and thresholds to mechanical stimulation were unaffected in the sham group 7 days after operation (Figure 2a). The TG Piezo2 mRNA expression level in the TN group was increased in

comparison with that in the sham group (Figure 2b), and the relative mRNA expression of Piezo2 was increased by approximately four-fold in the TN group. Moreover, TG Piezo2 expression at 21 days after operation was increased by twofold in the TN group in comparison with the sham group or naïve group (Figure 2c).

Double immunofluorescence labeling of Piezo2 with NSE and comparisons were made between different groups. The expression level of Piezo2 in the sham group rats was relatively low, but it remarkably increased in the TN group harvested 21 days after CCT (Figure 2d). Colocalization analysis revealed a Manders' Colocalization Coefficients (MCC) of 0.88 ± 0.02 for the sham group ($n = 6$) and 0.93 ± 0.02 for the TN group ($n = 6$). Besides the high colocalization coefficients, there is a significant correlation between the expression levels of Piezo2 and NSE, with a coefficient of determination (*R*) of 0.65 and 0.78 for the sham group and the TN group, respectively. Notably, the TN group has a regression slope of piezo2/NSE steeper than that of the sham group ($k = 1.22$ vs. 0.63) (Figure 2d). When the expression of Piezo2 in cell membrane and the cytoplasm were quantified separately, TN group displayed increased expression in both the cell membrane and the cytoplasm. (Figure 2e). Double immunofluorescence labeling of Piezo2 and NEFH (Figure 3a) showed that Piezo2 was remarkably increased in both NEFH-positive and NEFH-negative cells at 21 days after CCT. In the sham group, the fluorescence intensity was significantly higher in NEFH-positive cells than in NEFH-negative cells (Figure 3b). Piezo2 levels were remarkably increased in both CGRP-positive and CGRP-negative cells 21 days after CCT (Figure 3c–d).

3.2 | Piezo2 knockdown attenuated mechanical allodynia

Injection with LV-Piezo2 shRNA significantly attenuated CCT-induced mechanical allodynia (Figure 4a). Fluorescence from the exogenous marker protein ZsGreen was detected in TG tissue sections from the LV-Piezo2 shRNA and LV-scramble shRNA treatment groups 21 days after CCT (Figure 4b). Examination of Piezo2 fluorescence in the TN group, shRNA group, and scramble shRNA group 21 days after CCT showed that the fluorescence intensity of Piezo2 was lower than that in the TN group or scramble group. (Figure 4c). Western blot was performed to detect the knockdown efficiency of LV-Piezo2 shRNA (Figure 4d). LV-Piezo2 shRNA, but not the scramble shRNA, significantly reduced Piezo2 expression in the TG tissues under CCT treatment.

3.3 | The cAMP-Epac1 signaling pathway was up-regulated after CCT

At 21 days after the operation, the cAMP concentration in the sham group was approximately 30 nmol/L, but that in the TN group was increased to 40 nmol/L (Figure 5a). The results of qPCR showed the relative mRNA expression level of *Epac1* in the TN group

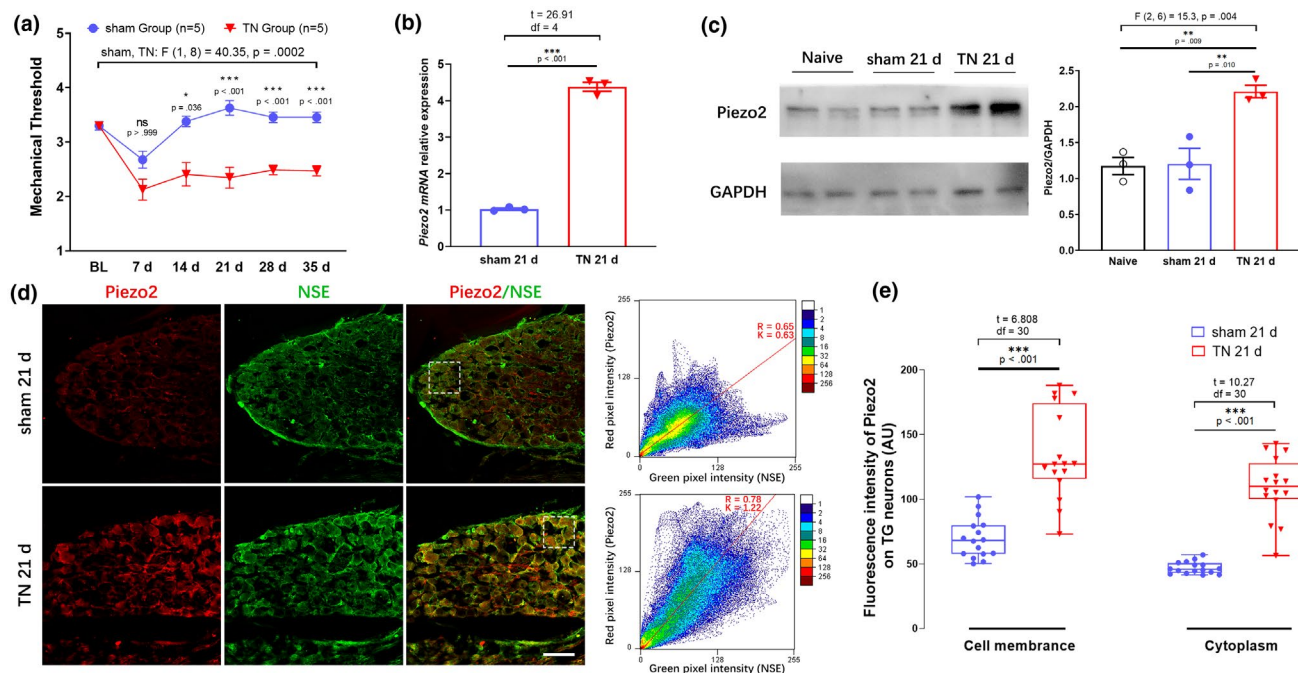


FIGURE 2 Chronic compression of the trigeminal nerve root (CCT) induced mechanical allodynia and up-regulated the expression of Piezo2. (a) CCT induced orofacial allodynia behaviors from 7 to 28 days after CCT (mean \pm SEM, $n = 5$, n indicates the number of independent animals; ns: no significant difference, $*p < 0.05$, $***p < 0.001$; two-way ANOVA). (b) *Piezo2* mRNA expression in the ipsilateral trigeminal ganglion (TG) from the sham group and trigeminal neuralgia (TN) group 21 days after operation. *Piezo2* expression was increased in the TN group after CCT (mean \pm SEM, $n = 3$, n indicates the number of independent animal TG RNA sample; $***p < 0.001$; unpaired *t*-test). (c) Western blot analysis showed an increase in *Piezo2* expression in the ipsilateral TG of the TN group 21 days after CCT. (mean \pm SEM, $n = 3$, n indicates the number of independent animal TG protein lysis; $*p < 0.05$, $**p < 0.01$; one-way ANOVA). (d) Representative images showing double immunostaining for *Piezo2* and neuron-specific enolase (NSE) in the TG. Each with the selected region quantified by Image J, showing a strong correlation of the immunoreactivity between *Piezo2* and NSE was analyzed in the selected area (dotted zone). Scale bar, 100 μ m. (e) Analysis of the *Piezo2* staining intensity in the cell membrane and somas of TG neurons showed that *Piezo2* levels were significantly increased in TG neurons after CCT ($n = 16$, n indicates the number of independent tissue slice from three animals; $**p < 0.01$, $***p < 0.001$; unpaired *t*-test). In the box-whisker plots, the bottom of each box is the 25th percentile, the top is the 75th percentile, and the line in the box is the median. The whisker above the box indicates the maximum and the whisker below the box indicates the minimum of these data, and the dots represent individual data

was increased by 1.5-fold compared with that in the sham group (Figure 5b). ATF3, a member of the cAMP-responsive element-binding (CREB) protein family of transcription factors, was remarkably increased in the nuclei of TG neurons compared with that in rats in the sham group (Figure 5c).

3.4 | P2Rs were up-regulated after CCT

Ipsilateral TREZ to TG tissues were harvested from the TN group and sham group 21 days after operation, and bulk RNA-seq was performed to obtain gene expression profiles which were normalized log₂ (FPKM+1) and false discovery rate (FDR) correction using Benjamini-Hochberg methods. The R (version 4.0.2) package DEGseq (ref: DEGseq: an R package for identifying differentially expressed genes from RNA-seq data) was used to identify 15 detected P2 genes (Figure 6a, b), five of which (*P2ry4*, *P2rx7*, *P2ry1*, *P2ry6*, and *P2ry14*) were up-regulated (a log₂FC ≥ 1 indicated differential expression) and another three (*P2rx2*, *P2ry2*, and *P2ry12*)

were down-regulated (a log₂FC ≤ -1 indicated differential expression) (Figure 6b). The qPCR results showed that the mRNA expression levels of *P2rx4*, *P2ry6*, *P2rx7*, *P2ry1*, *P2ry14*, *P2rx2*, *P2ry12*, and *P2ry2* in the TG were significantly up-regulated in the TN group compared with the sham group, while *P2ry12* mRNA expression was significantly down-regulated (Figure 6d). In particular, the relative expression of *P2ry2* was increased by ~threefold, that of *P2rx5* and *P2ry6* was increased by ~twofold, and that of *P2rx7* and *P2ry1* was increased by ~1.5-fold.

3.5 | Intracellular Ca²⁺ homeostasis in TG neurons were altered by ATP application

[Ca²⁺]_i in TG neurons was increased by application of ATP (final concentration of 1 mM), the initial rise in [Ca²⁺]_i was followed by a gradual decrease and returning to basal levels (Figure 7a). At 1mM ATP, there were no significant morphological changes (Figure 7b). However, some morphological changes might occur at higher ATP

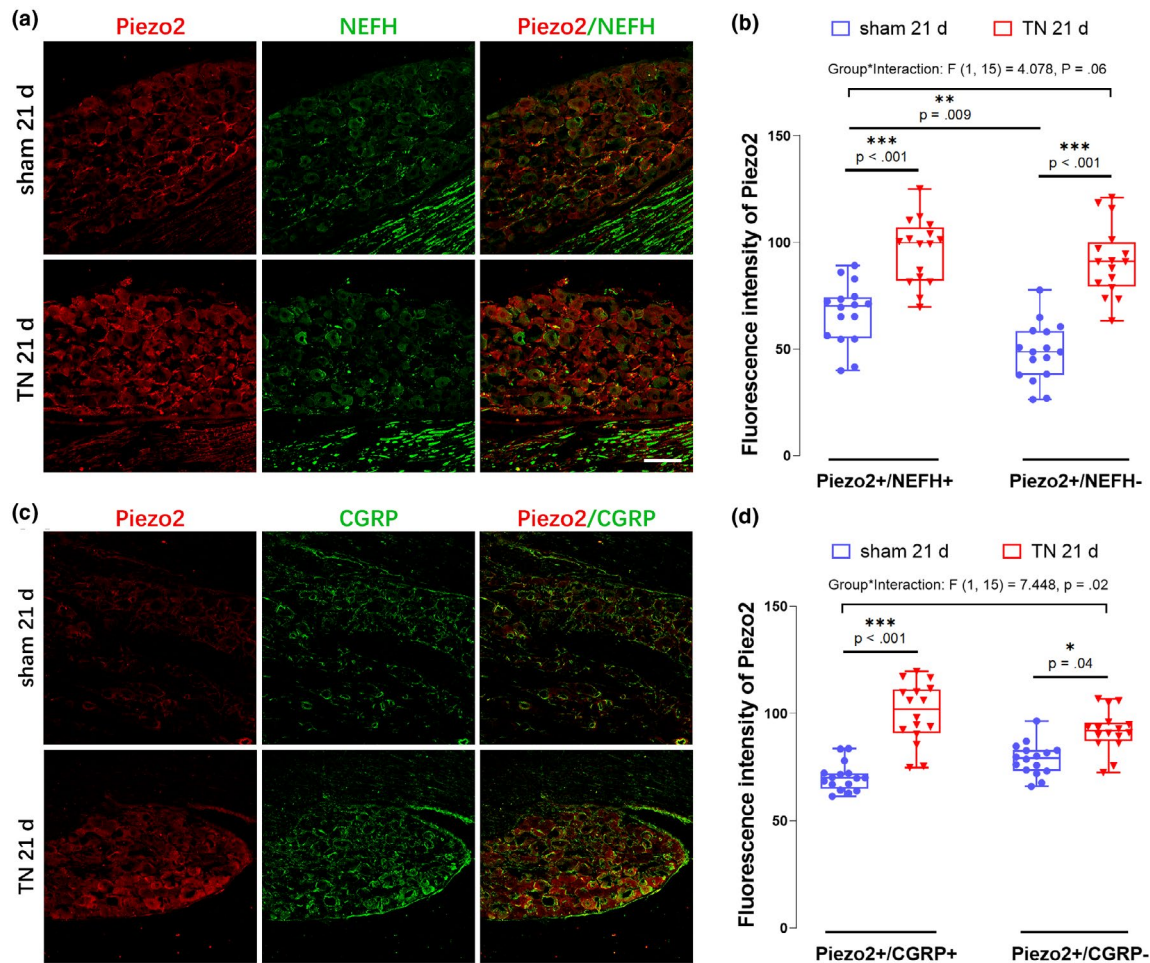


FIGURE 3 Cellular localization and expression patterns of Piezo2 in different subtypes of trigeminal ganglion (TG) neurons. (a) Double immunostaining for Piezo2/ neurofilament heavy chain (NEFH) in the TG. Scale bar, 100 μ m (b) The box-whisker plot shows the fluorescence intensity of Piezo2 in NEFH-positive and NEFH-negative cells in the sham group and TN group ($n = 16$, n indicates the number of independent tissue slice from four animals; $**p < 0.01$, $***p < 0.001$; two-way ANOVA). (c) Double immunostaining for Piezo2/ calcitonin gene-related peptide (CGRP) in the TG. Scale bar, 100 μ m. (d) The box-whisker plot shows the fluorescence intensity of Piezo2 in CGRP-positive and CGRP-negative cells in the sham group and trigeminal neuralgia (TN) group. The Piezo2 staining intensity was significantly increased in CGRP-negative cells and CGRP-positive cells after CCT ($n = 16$, n indicates the number of independent tissue slice from three animals; $*p < 0.05$, $***p < 0.001$; two-way ANOVA). In the box-whisker plots, the bottom of each box is the 25th percentile, the top is the 75th percentile, and the line in the box is the median. The whisker above the box indicates the maximum and the whisker below the box indicates the minimum of these data, and the dots represent individual data

levels and recovered after returning to an ATP-free culture medium (data not shown).

To exam the prolonged effect of ATP application on TG neurons, cells were treated with 3 mM ATP for 60min and then switched to a fresh culture medium for 3 days before $[Ca^{2+}]_i$ evaluation. Under identical dye and excitation parameters, TG neurons displayed higher basal 340/380 nm ratios, indicating higher initial $[Ca^{2+}]_i$. Because at resting conditions without mobilizing intracellular Ca^{2+} release, $[Ca^{2+}]_i$ is primarily set by the equilibrium of Ca^{2+} influx and Ca^{2+} efflux across the plasma membrane, the latter is largely dependent on the activity of Na^+/Ca^{2+} exchanger (NCX). Higher basal level $[Ca^{2+}]_i$ in ATP pre-treated TG neurons likely suggest increased influx or reduced efflux.

Ca^{2+} efflux mainly depends on the activity of Na^+/Ca^{2+} exchanger (NCX). In the presence of KB-R7943 (20 μ M) blocking a

majority of NCX activity, changes in $[Ca^{2+}]_i$ largely reflect Ca^{2+} influx (Figure 7c-d). The speed of $[Ca^{2+}]_i$ increase in ATP-pre-treated TG neurons is significantly higher than control cells pre-treatment on the regulation of $[Ca^{2+}]_i$ homeostasis in TG neurons. (Figure 7e).

3.6 | ATP pre-treatment increased mechanical stimulation-induced Ca^{2+} response in TG neurons

To evaluate ATP pre-treatment on the mechanical sensing by TG neurons in vitro, mechanical stimulation to TG neurons was applied by placing a layer of glass beads on top of the cultured TG neurons. Calculated from the size and density of the glass beads, a single layer of glass beads at the diameter of 100 μ m will likely deliver a

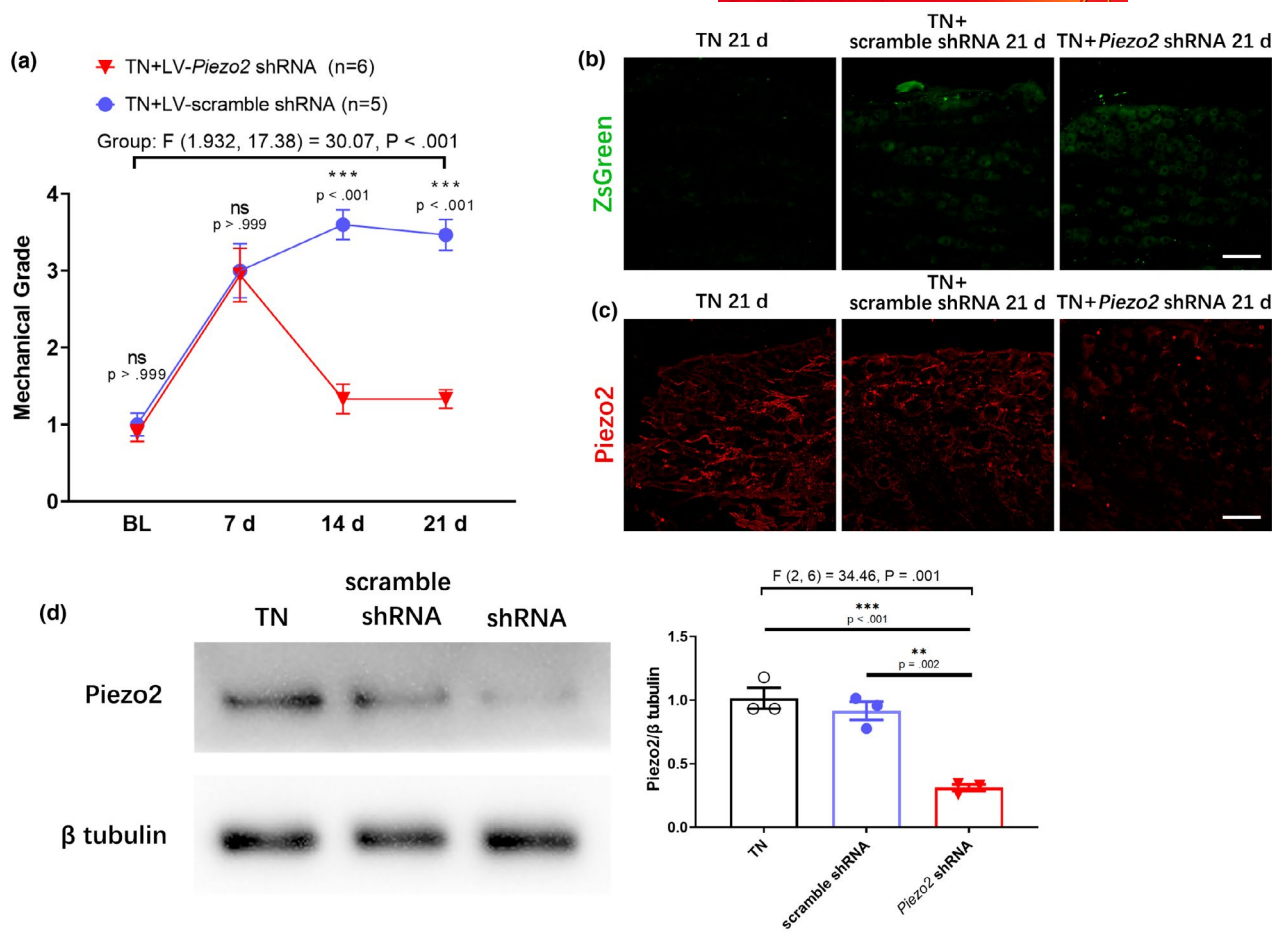


FIGURE 4 Effect of Piezo2 knockdown by shRNA on chronic compression of the trigeminal nerve root (CCT)-induced neuropathic pain. (a) CCT-induced mechanical allodynia was remarkably attenuated 14 days after CCT upon the intra-trigeminal ganglion (TG) injection of LV-*Piezo2* shRNA (mean \pm SEM, $n = 5$ or 6 , n indicates the number of independent animals; ns: no significant difference, *** $p < 0.001$; two-way ANOVA). (b) ZsGreen fluorescence was detected in the TG after the intra-TG injection of *Piezo2* shRNA and scramble shRNA. Scale bar, 100 μ m. (c) Representative image showing the ipsilateral TG from trigeminal neuralgia (TN) group, TN + *Piezo2* shRNA group and TN + scramble shRNA group. Scale bar, 100 μ m. (d) Knockdown of the Piezo2 protein was confirmed by Western blot analysis. Treatment with shRNA during the operation significantly reduced the expression level of Piezo2 in the TG 21 days after CCT. In addition, LV-Scramble shRNA did not affect Piezo2 expression in the TG (mean \pm SEM, $n = 3$, n indicates the number of independent animal TG protein lysis; ** $p < 0.01$, *** $p < 0.001$; one-way ANOVA)

mechanical pressure at around 10^{-5} atmosphere. Notably, at the initial stage, glass beads dropped through the aqueous layer, impacted the TG neurons with a momentum, and yielded a significantly higher mechanical stimulation.

Gentle application of glass beads triggered a huge initial rise of $[Ca^{2+}]_i$ in TG neurons followed by restoration to a new equilibrium level, accounted for the constant mechanical impact from the layer of glass beads, in a manner resembling tactile stimulation. Interestingly, the equilibrium level of $[Ca^{2+}]_i$ in TG neurons under the glass beads is different from the basal levels $[Ca^{2+}]_i$ before glass beads application (Figure 7b–c). For simplicity in comparison, glass bead application-induced alteration of intracellular Ca^{2+} level was termed as $\Delta[Ca^{2+}]_{i-gb}$. As shown in Figure 8, $\Delta[Ca^{2+}]_{i-gb}$ in ATP-treated TG neurons were significantly higher than those in naïve TG neurons (Figure 8a, c). Furthermore, the application of 3 μ M GsMTx4 (applied 30 min before and during Ca^{2+} imaging), a Piezo2

inhibitor, reduced a majority of the $\Delta[Ca^{2+}]_{i-gb}$ in ATP-treated TG neurons (Figure 8d–e).

3.7 | ATP up-regulated Piezo2 expression

To study the potential effort of ATP on the expression of Piezo2, immunofluorescence labeling of Piezo2 was performed on TG neurons 3 days after treated with 3 mM ATP and 500 nM ionomycin for 1 h. The representative images from the naïve group and ATP group showed ATP treated for 1 h significantly increased the expression of Piezo2. Treated with calcium ionophore ionomycin also induced a significant increase in Piezo2 (Figure 9a). The fluorescence intensities of Piezo2 in rats of the naïve group were relatively low, but that in the ATP group and the ionomycin group were remarkably increased (Figure 9b).

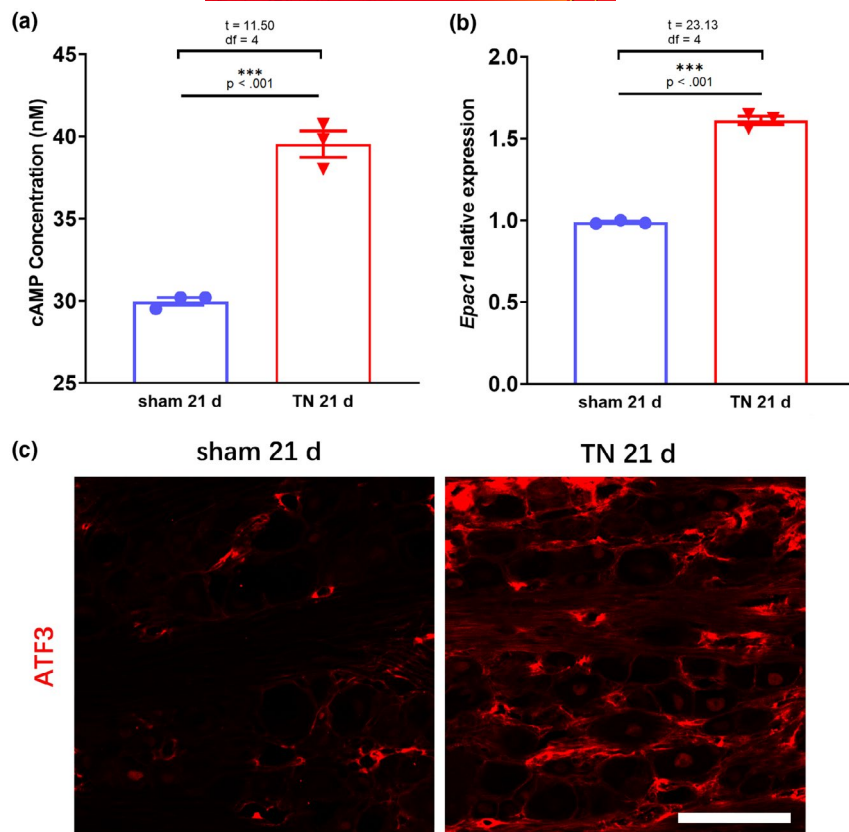


FIGURE 5 Chronic compression of the trigeminal nerve root (CCT) induced the activation of cyclic adenosine monophosphate-to-exchange protein directly activated by cAMP 1 (cAMP-to-Epac1) signaling in the trigeminal ganglion (TG). (a) Competitive ELISA showed the concentration of cAMP was remarkably increased in CCT-operated animals (mean \pm SEM, $n = 3$, n indicates the number of independent TG tissue; $***p < 0.001$; unpaired t-test). (b) CCT remarkably induced the up-regulation of Epac1 in the TG of rats in the TN group (mean \pm SEM, $n = 3$, n indicates the number of independent TG RNA sample; $***p < 0.001$; unpaired t-test). (c) The expression of activating transcription factor 3 (ATF3) in the TG of TN group rats was significantly increased compared with that from the sham group. Scale bar, 100 μ m

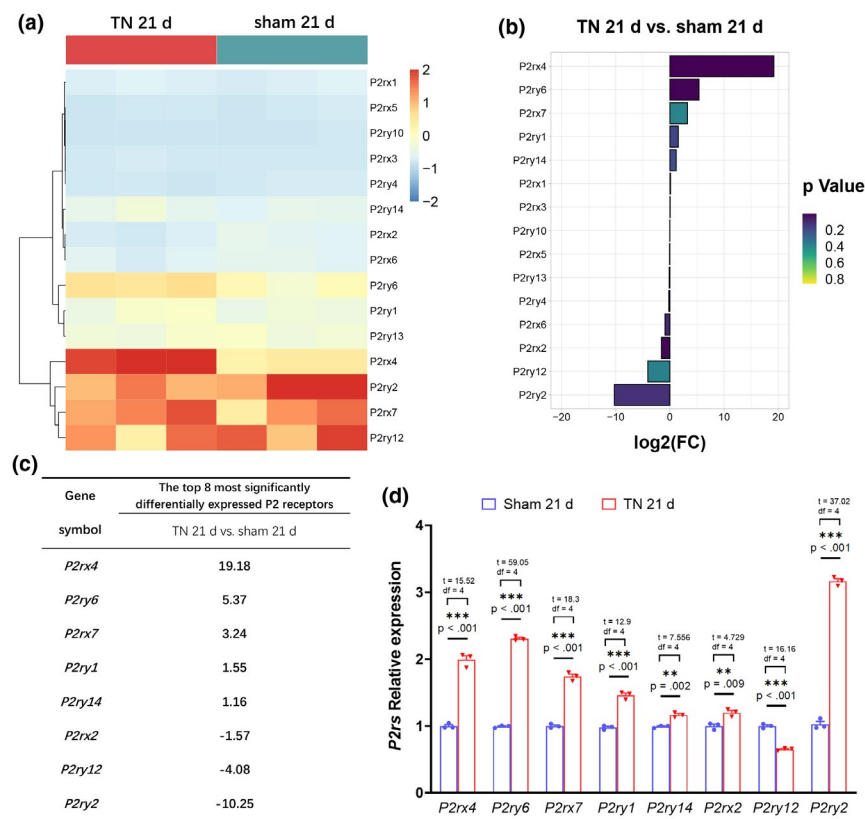


FIGURE 6 P2 receptor expression in the trigeminal ganglion (TG) was up-regulated after chronic compression of the trigeminal nerve root (CCT). (a) Heatmap of the expression of purinergic 2 receptors (P2Rs) in the TG 21 days after CCT based on bulk RNA-seq data. In the heatmap, red indicates up-regulated gene expression and blue indicated down-regulated gene expression. (b) Fold changes in up-regulated (log2FC > 0) and down-regulated (log2FC < 0) P2R genes at 21 days after CCT in the trigeminal neuralgia (TN) group compared with the sham group. (c) The top eight up-regulated and down-regulated genes in the TG after CCT were selected based on a fold change ≥ 1 . (d) Verification of P2rx4, P2ry6, P2rx7, P2ry1, P2ry14, P2rx2, P2ry12, and P2ry2 gene expression by qPCR (mean \pm SEM, $n = 3$, n indicates the number of independent TG RNA sample; $**p < 0.01$, $***p < 0.001$; unpaired t-test)

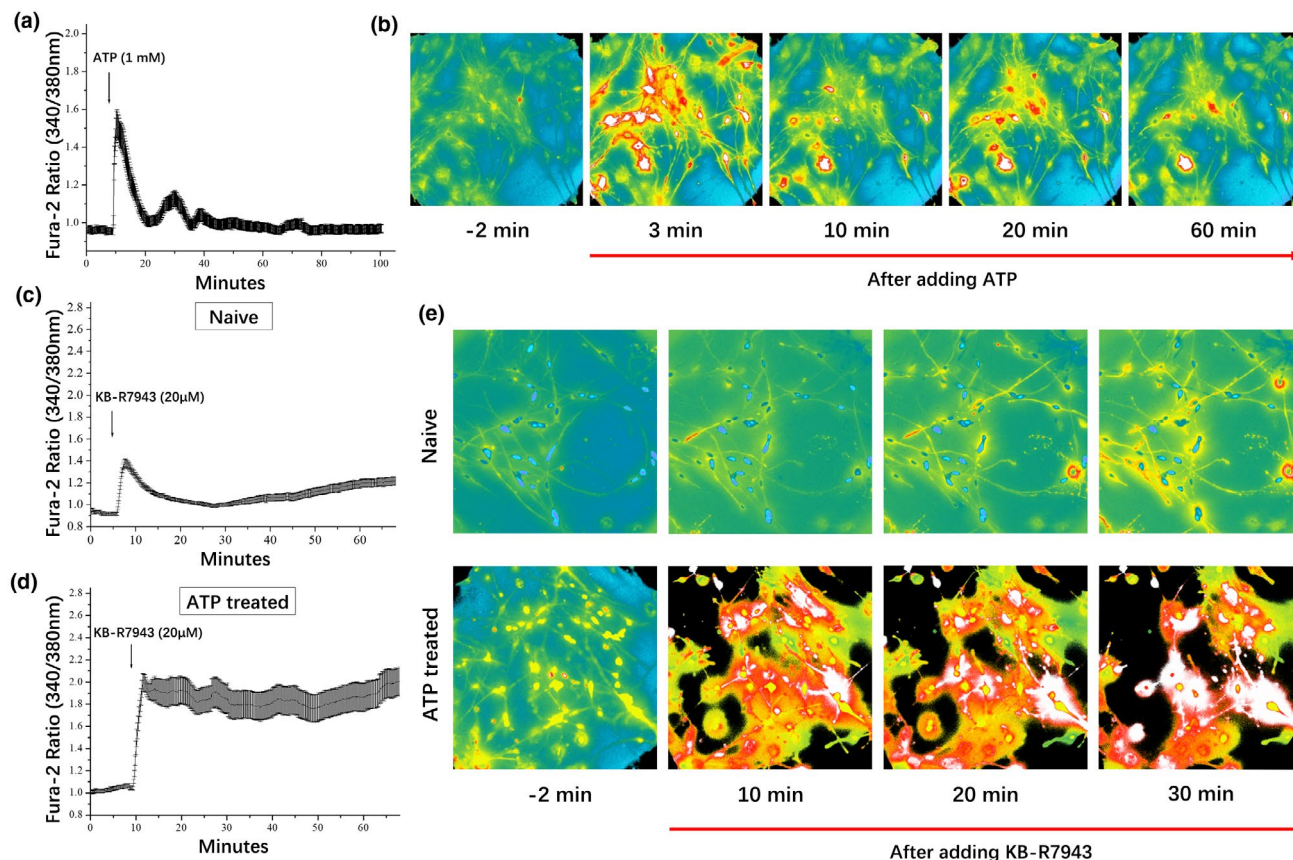


FIGURE 7 ATP induced a reversible $[Ca^{2+}]_i$ increase in cultured trigeminal ganglion (TG) neurons and ATP pre-treatment altered $[Ca^{2+}]_i$ homeostasis by making TG neurons more dependent on the function of Na^+/Ca^{2+} exchanger (NCX). (a) Fura-2 ratio after application of ATP to a final concentration of 1 mM. (b) Pseudocolored Fura-2 ratio images during the course of ATP stimulation. (c) Changes of Fura-2 ratios in naïve TG neurons upon receiving KB-R7943. (d) Changes in Fura-2 ratios in ATP pre-treated TG neurons upon receiving KB-R7943. (e) Fura-2 ratio images of control TG neurons and ATP pre-treated TG neurons after application of KB-R7943

4 | DISCUSSION

In this study, we observed a significant increase in Piezo2 expression in a CCT model of TN, along with the increase in multiple P2 receptors. Furthermore, ATP application increased Piezo2 expression in cultured TG neurons and elevated TG neuron sensitivity to tactile stimulation delivered by glass beads application.

Piezo2 is a specialized mechanosensitive ion channel that converts mechanical stimuli into electrochemical signals (Coste et al., 2010). The critical role of Piezo2 in mechanotransduction has been revealed in mechanoreceptors in the skin and primary sensory neurons (Coste et al., 2010; Feng et al., 2018). In the peripheral nervous system, Piezo2 mediates light touch and proprioception under physiological conditions (Neubarth et al., 2020; Woo et al., 2015), but under pathological conditions, such as nerve injury or inflammation, it mediates mechanical allodynia (Murthy et al., 2018b).

A study in which sensory neuron types were classified by single-cell RNA-seq revealed differences in the gene expression profiles of sensory neurons, which corresponded to the functions of neurons (Usoskin et al., 2015). It is generally believed that peptidergic and non-peptidergic C- and Aδ-fiber neurons convey noxious stimuli

from peripheral receptors, and thick, myelinated Aβ-fiber neurons convey innocuous stimuli (Basbaum et al., 2009; Djouhri & Lawson, 2004; Kwan et al., 2009). We initially suspected that the mechanical allodynia induced by CCT was related to changes in the expression level and distribution of Piezo2 in different subtypes of neurons. Piezo2 was up-regulated in most neurons in the TG, and the increase in Piezo2 was greater in CGRP-positive neurons, characterized by relatively smaller size in cell body and thinner myelination (Figure 3c, d). We hypothesized that CCT induced a widespread release of a signaling molecule that activated TG neurons, which subsequently up-regulate the expression of Piezo2 in nociceptive afferents. A previous study reported that not all sensory neurons in DRG were Piezo2 immunoreactive cells (Ranade et al., 2014), which was different from our results. This may likely be due to the potential difference between the TG and DRG. Additionally, it has been reported that different concentrations and formulations of PFA may affect the positive ratio of some ion channels on sensory neurons (Hoffman et al., 2010).

The finding of a significant increase in cAMP levels (Figure 5) is well in line with the increase in several P2Y receptors (Figure 6), which mostly linked to an increase in cAMP production (Zimmermann,

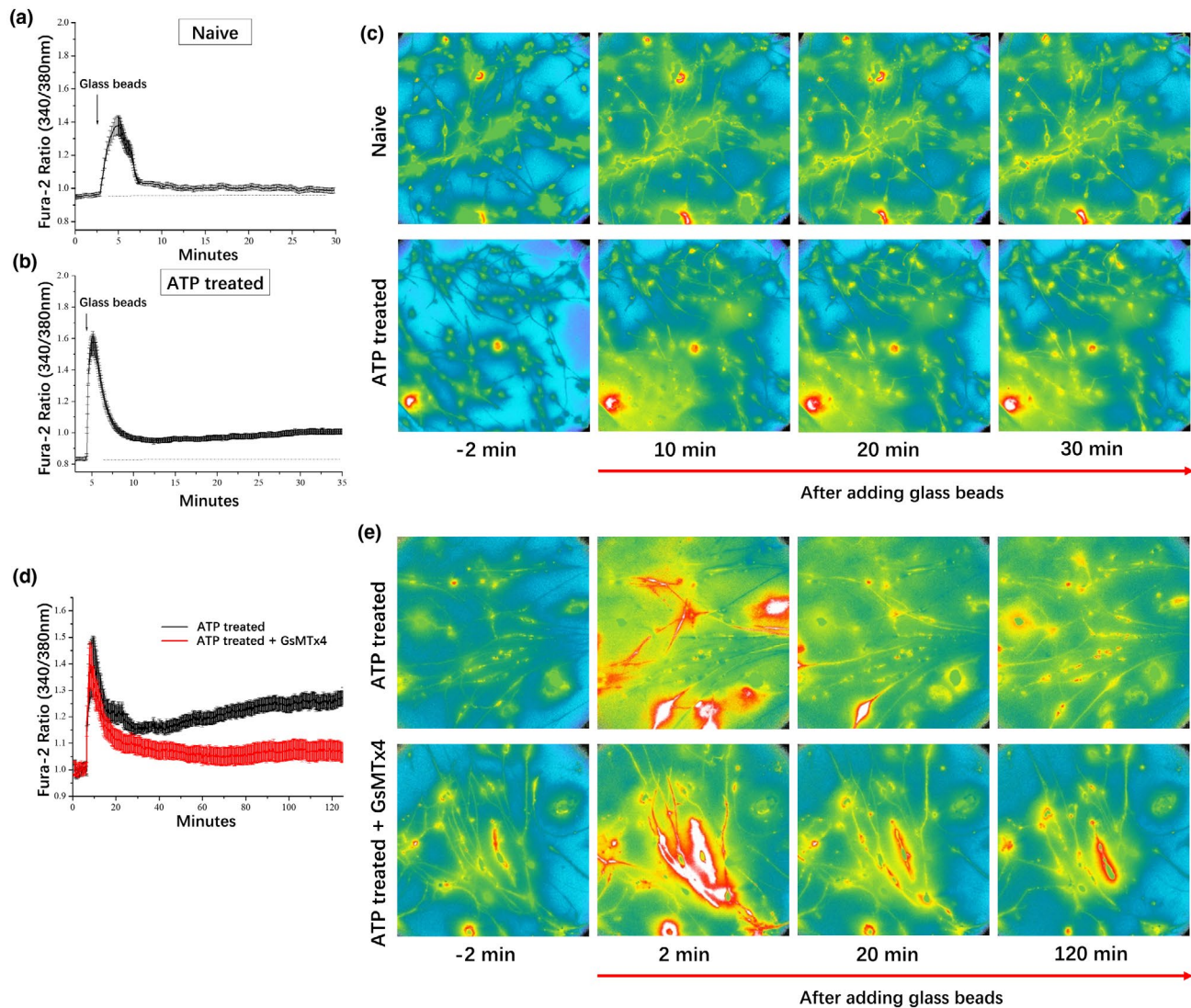


FIGURE 8 Mechanical stimulation induced a more sustainable $[Ca^{2+}]_i$ increase in trigeminal ganglion (TG) neurons pre-treated by ATP. (a) Glass beads application induced a $[Ca^{2+}]_i$ increase readily return to a steady level close to basal levels. (b) Glass beads application induced stronger and more sustainable $[Ca^{2+}]_i$ increase in ATP pre-treated TG neurons. (c) Fura-2 ratio images of the naïve and the ATP pre-treated TG neurons during the course of glass bead application. (d) GsMTx4 enabled the ATP pre-treated TG neurons a better restoration of $[Ca^{2+}]_i$ under the continuous pressure from glass beads. (e) Fura-2 ratio images of the ATP pre-treated TG neurons under glass beads in the absence or presence of GsMTx4

2016). An increase in cAMP facilitates the activation of Epac1, and the role of the cAMP-sensor protein Epac1 in long-lasting mechanical allodynia has been reported (Eijkelkamp et al., 2013). A significant increase in ATF3 expression was also observed a significant increase in the TN group. ATF3 is a marker of nerve injury and a member of the cAMP-responsive element-binding (CREB) protein family of transcription factors, which also indicates the activation of cAMP signaling.

The inflammatory mediator IL-6 induces the expression of Piezo2 (Liu et al., 2021). IL-1 α can up-regulate the expression of Piezo1 by activating p38 MAP-kinase and CREB (Lee et al., 2021). Moreover, extracellular ATP inhibits the dedifferentiation and proliferation of Schwann cells (Shin et al., 2013). In our TN animal model, demyelination and axon injury always occurred in the TREZ (Luo et al., 2012,

2019), which indicates the important role of ATP and P2Rs in TN, which is of significant clinical relevance, TN patients are often associated with demyelination and axon injury in the TREZ. It is well-known that nerve injury or compression is associated with strong ATP release (Liang et al., 2019; Masuda et al., 2016). Increasing evidence has also shown the role of P2Rs in neuropathic pain, and several drugs that antagonize P2Rs have been shown to decrease neuropathic pain (Burnstock, 2006; Tsuda, 2017; Zou et al., 2019). In this study, RNA-seq analysis showed that the expression of a variety of P2rs increased after CCT. We further performed qPCR to verify the expression levels of these P2rs. Several subtypes of P2Rs should be the interest to further studies.

In an in vitro study, we used a 60-min application of 3 mM ATP to pre-treat TG neurons in culture, which has provided a

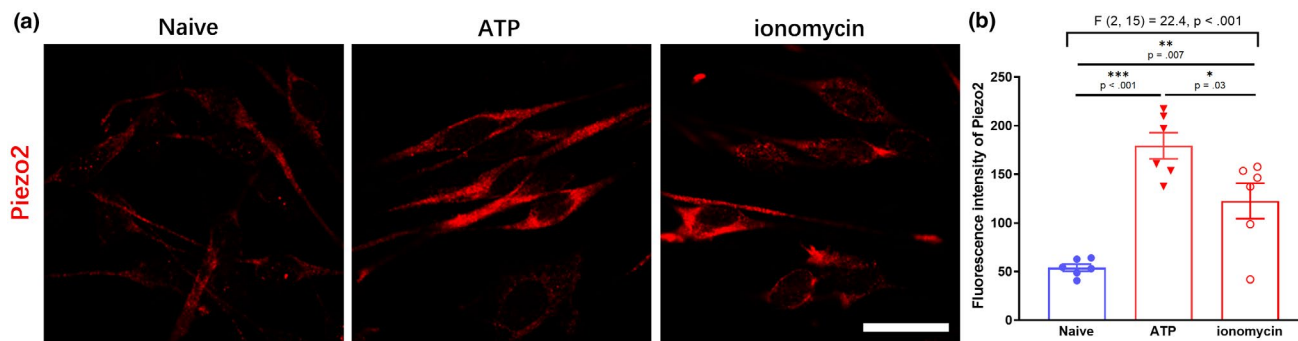


FIGURE 9 ATP up-regulated Piezo2 expression. (a) Immunostaining of Piezo2 in cultured trigeminal ganglion (TG) neurons after treatment with different drugs. Scale bar, 10 μ m. (b) The histogram shows the fluorescence intensity of Piezo2 in TG neurons in different groups. ATP and ionomycin significantly increased the expression level of Piezo2 (mean \pm SEM, $n = 6$, n indicates the number of independent cell culture preparations; * $p < 0.05$, ** $p < 0.01$, *** $p < 0.001$; One-way ANOVA)

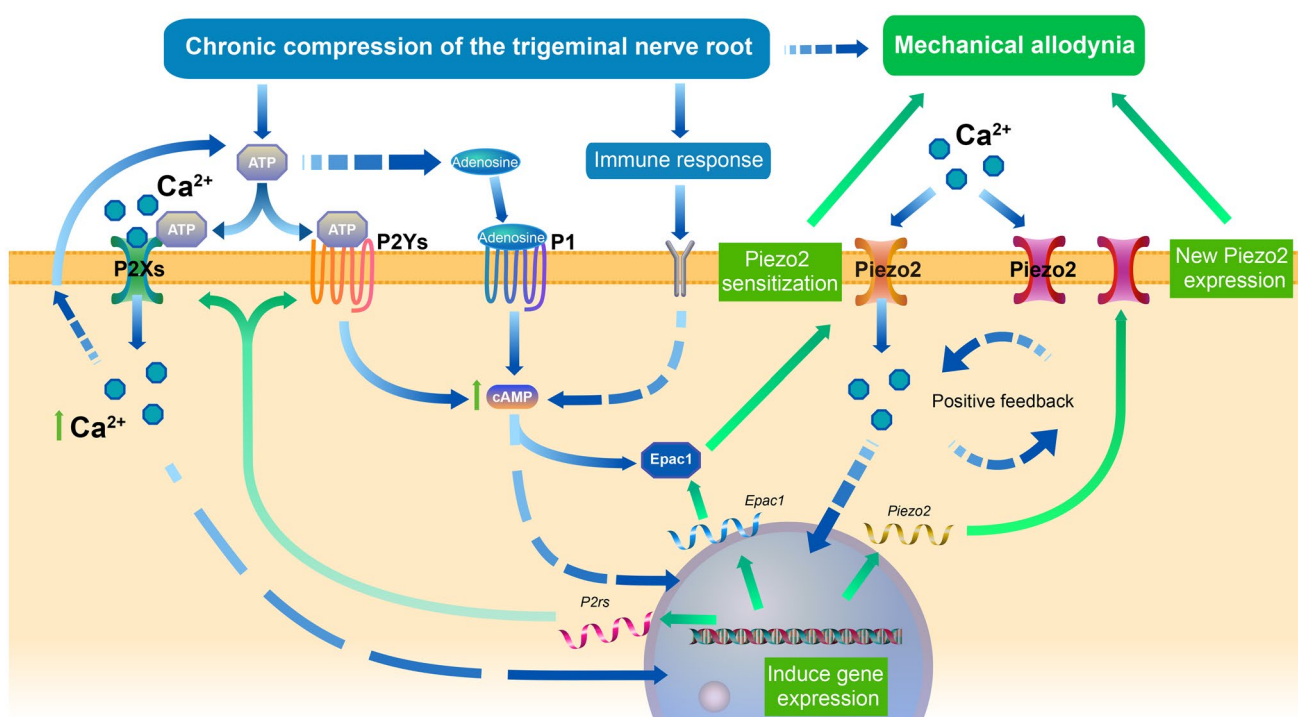


FIGURE 10 Schematic illustration of the mechanisms by which chronic compression of the trigeminal nerve root (CCT) promotes mechanical allodynia in TG neurons. During nerve injury, ATP is released from the injured tissue and activates the purinergic 2 receptors (P2Rs) on the cell membrane of TG neurons. Activation of the P2Rs increases the $[Ca^{2+}]_i$ and activates the Ca^{2+} signaling pathway, which leads to up-regulation of the expression of Piezo2. Meanwhile, intracellular cAMP is increased by activation of adenosine receptors (P1 receptors) and P2Y receptors, together with neuroimmune response. cAMP signaling potentiates the sensitivity of Piezo2 to mechanical stimulation through Epac1 pathway. In summary, Ca^{2+} -mediated increase in Piezo2 expression together with cAMP-mediated sensitization of Piezo2 synergistically increase the response of TG neurons to mechanical stimulation and initiate mechanical allodynia. Notably, over-expression and sensitization of Piezo2 increase influx of Ca^{2+} , during mechanical stimulation, inadvertently forms a positive feedback loop at stimulating Piezo2 expression, leads to the persistence of the mechanical allodynia

proof of principle that ATP is sufficient at inducing mechanical over-sensitization in vitro, or an in vitro form of tactile allodynia. Immunofluorescent study 3 days after ATP application revealed a significant increase in Piezo2 expression. Treating cells with 500 nM ionomycin for 1 h to induce Ca^{2+} influx also increased the expression of Piezo2 significantly, but not as much as ATP

did. Nevertheless, the ionomycin effect supports the notion that ATP-induced increase in $[Ca^{2+}]_i$ is essential in the signaling cascade leading to Piezo2 expression. Besides Ca^{2+} , ATP and adenosine also initiate other signaling cascade, such as cAMP that is involved in Piezo2 regulation (van Calcar et al., 2019; Dubin et al., 2012). The relative contribution of P1 receptors, P2X receptors, and P2Y

receptors in stimulation of Piezo2 express worth further detailed studies.

The existing results indicate that ATP is pivotal at up-regulating Piezo2 expression and alter Ca^{2+} homeostasis in TG neurons. ATP pre-treated TG neurons displayed a prominent sensitivity to mechanical stimulation, manifested as higher $[\text{Ca}^{2+}]_i$ in responding to tactile stimulation from glass beads. We estimated that the mechanical pressure sensed by the nerve terminals, when delivered by the finest von Frey filament that was sufficient to induce avoidance response, at around 8–70 mg (D. S. Luo et al., 2012), was in the same magnitude as the pressure generated by about 15 mg of glass beads evenly distributed to an area of approximately 50–100 mm^2 . After the initial momentum, the glass beads delivered a steady mechanical pressure in the magnitude of 10^{-5} – 10^{-4} atmosphere. Notably, only ATP-treated TG neurons responded to such stimulation with a significant increase in the equilibrium $[\text{Ca}^{2+}]_i$ levels, termed as $\Delta[\text{Ca}^{2+}]_{i-\text{gb}}$. Monitoring the $[\text{Ca}^{2+}]_i$ in TG neurons in responding to glass beads application may provide an in vitro paradigm to mimic in vivo tactile allodynia.

During CCT, the released ATP is most likely at sub-mM level, but the duration of ATP release is expected to be long-lasting. ATP activation of P2Y and P1 receptors leads to increases in cAMP level and Epac1-dependent Piezo2 potentiation, making mechanical stimulation more likely to induce Ca^{2+} influx into TG neurons. Ca^{2+} influx stimulates Piezo2 expression and may form a positive feedback loop in the presence of mechanical stimulation. This positive feedback is further fortified by Ca^{2+} -dependent ATP release (Lezmy et al., 2021) and contributes significantly to the pathogenesis of mechanical allodynia.

5 | CONCLUSIONS

As summarized in a schematic drawing (Figure 10), this study reported a significant increase in the expression of multiple ATP receptors and Piezo2 in a TN animal model. ATP application to cultured TG neurons could induce Piezo2 expression and increase sensitivity to mechanical stimuli. These results indicate a pivotal role of ATP signaling, Ca^{2+} influx, cAMP, and Piezo2 expression in the pathogenesis of mechanical allodynia.

ACKNOWLEDGMENTS

We thank Ling Lin (Public Technology Service Center of Fujian Medical University) for microscopic imaging technology support, Shaowei Lin (School of Public Health of Fujian Medical University) for providing advice with statistical testing, and Haoyuan Shi (Fujian Medical University) for assistance with bioinformatic analysis. This work was funded by the National Natural Science Foundation of China (Grant number: 82171213), United Fujian Provincial Health and Education Project for Tackling the Key Research P.R. China (Grant number: 2019WJ26) and Startup Fund for scientific research, Fujian Medical University (Grant number: 2020QH1001).

All experiments were conducted in compliance with the ARRIVE guidelines.

CONFLICT OF INTEREST

The authors declare that there is no conflict of interest.

AUTHORS' CONTRIBUTIONS

Zhaoke Luo and Xinyue Liao performed TN animal model operation, behavior test, cell culture, morphological study, experiment of molecular biology, and data analysis. Zhaoke Luo drafted the manuscript. Lili Luo carried out cell intervention experiments and functional imaging experiments. Qitong Fan helped to set up TN animal model and provided TG neurons primary culture technology. Xiaofeng Zhang helped during set up TN animal model and helped to feed animals. Yuefeng Guo and Feng Wang assisted in the qPCR experiments. Zucheng Ye provided an experimental scheme of cell intervention, functional imaging experiment, data analysis, and guidance on draft. Daoshu Luo designed the experiment, analyzed the data, revised the manuscript, and responded to the journal.

OPEN RESEARCH BADGES



This article has earned an Open Materials badge for making publicly available the components of the research methodology needed to reproduce the reported procedure and analysis.

DATA AVAILABILITY STATEMENT

The data that support the findings of this study are available from the corresponding author upon reasonable request.

ORCID

Yuefeng Guo <https://orcid.org/0000-0002-3327-621X>

Daoshu Luo <https://orcid.org/0000-0001-9013-1052>

REFERENCES

- Basbaum, A. I., Bautista, D. M., Scherrer, G., & Julius, D. (2009). Cellular and molecular mechanisms of pain. *Cell*, 139(2), 267–284. <https://doi.org/10.1016/j.cell.2009.09.028>.
- Bernier, L. P., Ase, A. R., & Séguéla, P. (2018). P2X receptor channels in chronic pain pathways. *British Journal of Pharmacology*, 175(12), 2219–2230. <https://doi.org/10.1111/bph.13957>.
- Borbiro, I., Badheka, D., & Rohacs, T. (2015). Activation of TRPV1 channels inhibits mechanosensitive Piezo channel activity by depleting membrane phosphoinositides. *Science Signaling*, 8(363), ra15. <https://doi.org/10.1126/scisignal.2005667>.
- Burnstock, G. (1972). Purinergic nerves. *Pharmacological Reviews*, 24(3), 509–581.
- Burnstock, G. (2006). Purinergic P2 receptors as targets for novel analgesics. *Pharmacology & Therapeutics*, 110(3), 433–454. <https://doi.org/10.1016/j.pharmthera.2005.08.013>.
- Burnstock, G. (2012). Purinergic signalling: Its unpopular beginning, its acceptance and its exciting future. *BioEssays*, 34(3), 218–225. <https://doi.org/10.1002/bies.201100130>.
- Chesler, A. T., Szczot, M., Bharucha-Goebel, D., Čeko, M., Donkervoort, S., Laubacher, C., Hayes, L. H., Alter, K., Zampieri, C., Stanley, C., Innes,

- A. M., Mah, J. K., Grosmann, C. M., Bradley, N., Nguyen, D., Foley, A. R., le Pichon, C. E., & Bönnemann, C. G. (2016). The role of PIEZO2 in human mechanosensation. *New England Journal of Medicine*, 375(14), 1355–1364. <https://doi.org/10.1056/NEJMoa1602812>.
- Coste, B., Mathur, J., Schmidt, M., Earley, T. J., Ranade, S., Petrus, M. J., Dubin, A. E., & Patapoutian, A. (2010). Piezo1 and Piezo2 are essential components of distinct mechanically activated cation channels. *Science*, 330(6000), 55–60. <https://doi.org/10.1126/science.1193270>.
- Crucchi, G., Finnerup, N. B., Jensen, T. S., Scholz, J., Sindou, M., Svensson, P., Treede, R.-D., Zakrzewska, J. M., & Nurmikko, T. (2016). Trigeminal neuralgia: New classification and diagnostic grading for practice and research. *Neurology*, 87(2), 220–228. <https://doi.org/10.1212/WNL.0000000000002840>.
- Djouhri, L., & Lawson, S. N. (2004). A β -fiber nociceptive primary afferent neurons: a review of incidence and properties in relation to other afferent A-fiber neurons in mammals. *Brain Research Reviews*, 46(2), 131–145. <https://doi.org/10.1016/j.brainresrev.2004.07.015>.
- Dubin, A. E., Schmidt, M., Mathur, J., Petrus, M. J., Xiao, B., Coste, B., & Patapoutian, A. (2012). Inflammatory signals enhance Piezo2-mediated mechanosensitive currents. *Cell Reports*, 2(3), 511–517. <https://doi.org/10.1016/j.celrep.2012.07.014>.
- Eijkelkamp, N., Linley, J. E., Torres, J. M., Bee, L., Dickenson, A. H., Gringhuis, M., Minett, M. S., Hong, G. S., Lee, E., Oh, U., Ishikawa, Y., Zwartkuis, F. J., Cox, J. J., & Wood, J. N. (2013). A role for Piezo2 in EPAC1-dependent mechanical allodynia. *Nature Communications*, 4(1), 1682. <https://doi.org/10.1038/ncomms2673>.
- Feng, J., Luo, J., Yang, P., Du, J., Kim, B. S., & Hu, H. (2018). Piezo2 channel-Merkel cell signaling modulates the conversion of touch to itch. *Science*, 360(6388), 530–533. <https://doi.org/10.1126/science.aar5703>.
- Hoffman, E. M., Schechter, R., & Miller, K. E. (2010). Fixative composition alters distributions of immunoreactivity for glutaminase and two markers of nociceptive neurons, Nav1.8 and TRPV1, in the rat dorsal root ganglion. *Journal of Histochemistry and Cytochemistry*, 58(4), 329–344. <https://doi.org/10.1369/jhc.2009.954008>.
- Jia, Z., Ikeda, R., Ling, J., & Gu, J. G. (2013). GTP-dependent run-up of Piezo2-type mechanically activated currents in rat dorsal root ganglion neurons. *Molecular Brain*, 6(1), 1–8. <https://doi.org/10.1186/1756-6606-6-57>.
- Jiang, B.-C., Zhang, J., Wu, B., Jiang, M., Cao, H., Wu, H., & Gao, Y.-J. (2021). G protein-coupled receptor GPR151 is involved in trigeminal neuropathic pain via the induction of G β γ /ERK-mediated neuroinflammation in the trigeminal ganglion. *Pain*, 162(5), 1434–1448. <https://doi.org/10.1097/j.pain.0000000000002156>.
- Jones, M. R., Urits, I., Ehrhardt, K. P., Cefalu, J. N., Kendrick, J. B., Park, D. J., Cornett, E. M., Kaye, A. D., & Viswanath, O. (2019). A comprehensive review of trigeminal neuralgia. *Current Pain and Headache Reports*, 23(10), 1–7. <https://doi.org/10.1007/s11916-019-0810-0>.
- Kwan, K. Y., Glazer, J. M., Corey, D. P., Rice, F. L., & Stucky, C. L. (2009). TRPA1 modulates mechanotransduction in cutaneous sensory neurons. *Journal of Neuroscience*, 29(15), 4808–4819. <https://doi.org/10.1523/JNEUROSCI.5380-08.2009>.
- Lee, W., Nims, R. J., Savadipour, A., Zhang, Q., Leddy, H. A., Liu, F., McNulty, A. L., Chen, Y., Guilak, F., & Liedtke, W. B. (2021). Inflammatory signaling sensitizes Piezo1 mechanotransduction in articular chondrocytes as a pathogenic feed-forward mechanism in osteoarthritis. *Proceedings of the National Academy of Sciences of the United States of America*, 118(13), 1–10. <https://doi.org/10.1073/pnas.2001611118>.
- Lezmy, J., Arancibia-Cárcamo, I. L., Quintela-López, T., Sherman, D. L., Brophy, P. J., & Attwell, D. (2021). Astrocyte Ca $^{2+}$ -evoked ATP release regulates myelinated axon excitability and conduction speed. *Science (New York, N.Y.)*, 374(6565), eabh2858. <https://doi.org/10.1126/science.abh2858>.
- Liang, Y., Gu, Y., Shi, R., Li, G., Chen, Y., & Huang, L. Y. M. (2019). Electroacupuncture downregulates P2X3 receptor expression in dorsal root ganglia of the spinal nerve-ligated rat. *Molecular Pain*, 15, 1–10. <https://doi.org/10.1177/1744806919847810>.
- Lin, R., Luo, L., Gong, Y., Zheng, J., Wang, S., Du, J., & Luo, D. (2019). Immunohistochemical analysis of histone H3 acetylation in the trigeminal root entry zone in an animal model of trigeminal neuralgia. *Journal of Neurosurgery*, 131(3), 8–11. <https://doi.org/10.3171/2018.5.JNS172948>.
- Liu, M., Li, Y., Zhong, J., Xia, L., & Dou, N. (2021). The effect of IL-6/Piezo2 on the trigeminal neuropathic pain. *Aging*, 13, 1–11. <https://doi.org/10.18632/aging.202887>.
- Luo, D. S., Lin, R., Luo, L. L., Li, Q. H., Chen, T., Qiu, R. H., & Li, Y. Q. (2019). Glial plasticity in the trigeminal root entry zone of a rat trigeminal neuralgia animal model. *Neurochemical Research*, 44(8), 1893–1902. <https://doi.org/10.1007/s11064-019-02824-2>.
- Luo, D. S., Zhang, T., Zou, C. X., Zuo, Z. F., Li, H., Wu, S. X., Wang, W., & Li, Y. Q. (2012). An animal model for trigeminal neuralgia by compression of the trigeminal nerve root. *Pain Physician*, 15(2), 187–196.
- Masuda, T., Ozono, Y., Mikuriya, S., Kohro, Y., Tozaki-Saitoh, H., Iwatsuki, K., Uneyama, H., Ichikawa, R., Salter, M. W., Tsuda, M., & Inoue, K. (2016). Dorsal horn neurons release extracellular ATP in a VNUT-dependent manner that underlies neuropathic pain. *Nature Communications*, 7, 12529. <https://doi.org/10.1038/ncomms12529>.
- Murthy, S. E., Loud, M. C., Daou, I., Marshall, K. L., Schwaller, F., Kühnemund, J., Francisco, A. G., Keenan, W. T., Dubin, A. E., Lewin, G. R., & Patapoutian, A. (2018a). The mechanosensitive ion channel Piezo2 mediates sensitivity to mechanical pain in mice. *Science Translational Medicine*, 10(462), eaat9897. <https://doi.org/10.1126/scitranslmed.aat9897>.
- Murthy, S. E., Loud, M. C., Daou, I., Marshall, K. L., Schwaller, F., Kühnemund, J., Francisco, A. G., Keenan, W. T., Dubin, A. E., Lewin, G. R., & Patapoutian, A. (2018b). The mechanosensitive ion channel Piezo2 mediates sensitivity to mechanical pain in mice. *Science Translational Medicine*, 10(462), eaat9897. <https://doi.org/10.1126/scitranslmed.aat9897>.
- Neubarth, N. L., Emanuel, A. J., Liu, Y., Springel, M. W., Handler, A., Zhang, Q., Lehnert, B. P., Guo, C., Orefice, L. L., Abdelaziz, A., DeLisle, M. M., Iskols, M., Rhyins, J., Kim, S. J., Cattel, S. J., Regehr, W., Harvey, C. D., Drugowitsch, J., & Ginty, D. D. (2020). Meissner corpuscles and their spatially intermingled afferents underlie gentle touch perception. *Science*, 368(6497), <https://doi.org/10.1126/science.abb2751>.
- Petit, P., Lajoix, A.-D., & Gross, R. (2009). P2 purinergic signalling in the pancreatic β -cell: Control of insulin secretion and pharmacology. *European Journal of Pharmaceutical Sciences*, 37(2), 67–75. <https://doi.org/10.1016/j.ejps.2009.01.007>.
- Ranade, S. S., Woo, S. H., Dubin, A. E., Moshourab, R. A., Wetzel, C., Petrus, M., Mathur, J., Bégay, V., Coste, B., Mainquist, J., Wilson, A. J., Francisco, A. G., Reddy, K., Qiu, Z., Wood, J. N., Lewin, G. R., & Patapoutian, A. (2014). Piezo2 is the major transducer of mechanical forces for touch sensation in mice. *Nature*, 516(729), 121–125. <https://doi.org/10.1038/nature13980>.
- Schmid, R., & Evans, R. J. (2019). ATP-gated P2X receptor channels: molecular insights into functional roles. *Annual Review of Physiology*, 81(1), 43–62. <https://doi.org/10.1146/annurev-physiol-020518-114259>.
- Shin, Y. H., Lee, S. J., & Jung, J. (2013). Extracellular ATP inhibits Schwann cell differentiation and proliferation in an ex vivo model of Wallerian degeneration. *Biochemical and Biophysical Research Communications*, 430(2), 852–857. <https://doi.org/10.1016/j.bbrc.2012.11.057>.
- Szczot, M., Liljencrantz, J., Ghitani, N., Barik, A., Lam, R., Thompson, J. H., Bharucha-Goebel, D., Saade, D., Necaie, A., Donkersvoort, S., Foley, A. R., Gordon, T., Case, L., Bushnell, M. C., Bönnemann, C. G., & Chesler, A. T. (2018). PIEZO2 mediates injury-induced tactile pain in mice and humans. *Science Translational Medicine*, 10(462), 1–10. <https://doi.org/10.1126/scitranslmed.aat9892>.
- Tsuda, M. (2017). P2 receptors, microglial cytokines and chemokines, and neuropathic pain. *Journal of Neuroscience Research*, 95(6), 1319–1329. <https://doi.org/10.1002/jnr.23816>.
- Usoskin, D., Furlan, A., Islam, S., Abdo, H., Lönnerberg, P., Lou, D., Hjerling-Leffler, J., Haeggström, J., Kharchenko, O., Kharchenko, P.



- V., Linnarsson, S., & Ernfors, P. (2015). Unbiased classification of sensory neuron types by large-scale single-cell RNA sequencing. *Nature Neuroscience*, 18(1), 145–153. <https://doi.org/10.1038/nn.3881>.
- van Calker, D., Biber, K., Domschke, K., & Serchov, T. (2019). The role of adenosine receptors in mood and anxiety disorders. *Journal of Neurochemistry*, 151(1), 11–27. <https://doi.org/10.1111/jnc.14841>.
- Woo, S. H., Lumpkin, E. A., & Patapoutian, A. (2015). Merkel cells and neurons keep in touch. *Trends in Cell Biology*, 25(2), 74–81. <https://doi.org/10.1016/j.tcb.2014.10.003>.
- Yao, P. S., Kang, D. Z., Lin, R. Y., Ye, B., Wang, W., & Ye, Z. C. (2014). Glutamate/glutamine metabolism coupling between astrocytes and glioma cells: Neuroprotection and inhibition of glioma growth. *Biochemical and Biophysical Research Communications*, 450(1), 295–299. <https://doi.org/10.1016/j.bbrc.2014.05.120>.
- Zimmermann, H. (2016). Extracellular ATP and other nucleotides—ubiquitous triggers of intercellular messenger release. *Purinergic Signalling*, 12(1), 25–57. <https://doi.org/10.1007/s11302-015-9483-2>.
- Zou, L., Gong, Y., Liu, S., & Liang, S. (2019). Natural compounds acting at P2 receptors alleviate peripheral neuropathy. *Brain Research*

Bulletin, 151, 125–131. <https://doi.org/10.1016/j.brainresbull.2018.12.017>.

SUPPORTING INFORMATION

Additional supporting information may be found in the online version of the article at the publisher's website.

How to cite this article: Luo, Z., Liao, X., Luo, L., Fan, Q., Zhang, X., Guo, Y., Wang, F., Ye, Z., & Luo, D. (2021). Extracellular ATP and cAMP signaling promote Piezo2-dependent mechanical allodynia after trigeminal nerve compression injury. *Journal of Neurochemistry*, 00, 1–16. <https://doi.org/10.1111/jnc.15537>